Journal of Solid State Chemistry 213 (2014) 145–151

Contents lists available at ScienceDirect

Journal of Solid State Chemistry

journal homepage: www.elsevier.com/locate/jssc

The role of SO_4^{2-} surface distribution in arsenic removal by iron oxy-hydroxides

S. Tresintsi [a], K. Simeonidis [a,b,*], N. Pliatsikas [c], G. Vourlias [c], P. Patsalas [c], M. Mitrakas [a]

[a] Analytical Chemistry Laboratory, Department of Chemical Engineering, Aristotle University of Thessaloniki, 54124 Thessaloniki, Greece
[b] Department of Mechanical Engineering, University of Thessaly, 38334 Volos, Greece
[c] Laboratory of Applied Physics, Department of Physics, Aristotle University of Thessaloniki, 54124 Thessaloniki, Greece

ARTICLE INFO

Article history:
Received 27 November 2013
Received in revised form
29 January 2014
Accepted 17 February 2014
Available online 24 February 2014

Keywords:
Sulfate
Iron oxy-hydroxides
Arsenic adsorption
XPS
FTIR

ABSTRACT

This study investigates the contribution of chemisorbed SO_4^{2-} in improving arsenic removal properties of iron oxy-hydroxides through an ion-exchange mechanism. An analytical methodology was developed for the accurate quantification of sulfate ion (SO_4^{2-}) distribution onto the surface and structural compartments of iron oxy-hydroxides synthesized by $FeSO_4$ precipitation. The procedure is based on the sequential determination of SO_4^{2-} presence in the diffuse and Stern layers, and the structure of these materials as defined by the sulfate-rich environments during the reaction and the variation in acidity (pH 3–12). Physically sorbed SO_4^{2-}, extracted in distilled water, and physically/chemically adsorbed ions on the oxy-hydroxide's surface leached by a 5 mM NaOH solution, were determined using ion chromatography. Total sulfate content was gravimetrically measured by precipitation as $BaSO_4$. To validate the suggested method, results were verified by X-ray photoelectron and Fourier-transformed infrared spectroscopy. Results showed that low precipitation pH-values favor the incorporation of sulfate ions into the structure and the inner double layer, while under alkaline conditions ions shift to the diffuse layer.

1. Introduction

Sulfate (SO_4^{2-}) anions are very common in a variety of aqueous industrial and environmental processes [1,2]. In chemical reactions, sulfate ions mostly originate from the addition of H_2SO_4 to control acidity or the dissolution of sulfate salts (e.g. $CuSO_4$, $FeSO_4$, etc) in order to release a number of metal ions. In the latter case, relatively large concentrations of sulfates, equal to the corresponding metal ions, are present during the occurring reaction but do not participate on its progress. However, under certain conditions (pH, redox, temperature), a sulfate-rich environment may contribute to the determination of final products or the formation of by-products with released cations. Precipitation of metal oxides and hydroxides by their corresponding sulfate salts is a representative example [3,4]. The growth of such materials in the presence of high concentrations of sulfate ions may favor their strong adsorption on the solid surfaces or even their incorporation into the crystal structure [5]. Their affinity to the prepared metal oxy-hydroxides, together with their charge and ionic volume compared to other common ions (Cl^- or NO_3^-) can seriously modify the physicochemical properties of the obtained solid (specific surface, isoelectric point, density) [6].

Accordingly, knowledge of the role of sulfate ions in many industrial precipitation processes is essential to optimize materials technological properties and reduce production costs. For instance, the synthesis of iron oxy-hydroxides, the most common class of adsorbents used for arsenic removal, is carried out at industrial scale by precipitation of $FeSO_4$ or $FeCl_2$ under acidic or alkaline conditions [7]. As recently described, high concentrations of SO_4^{2-} originating from used ferrous salts play an important role in the phase and morphology of the final product. In addition, there are strong indications that arsenic removal efficiency is related to the presence of sulfate ions chemically adsorbed in the surface charge layer (Stern layer) of oxy-hydroxide surfaces through an ion-exchange mechanism [8]. Therefore, it would be beneficial not only to determine the total sulfate content but also to ascertain the accurate distribution of SO_4^{2-} in the various structure and surface compartments of the grains [9].

A number of procedures have been applied to determine SO_4^{2-} in solid materials. Of these, gravimetric [10], nephelometric [11], colorimetric [12] and ion chromatographic [13–15] methods are the most important, but the most common methods used are ion chromatography and the gravimetric method through the precipitation of $BaSO_4$. Ion chromatography with suppressed conductivity provides high sensitivity, regardless of whether the species

* Corresponding author at: Department of Mechanical Engineering, University of Thessaly, 38334 Volos, Greece. Tel./fax +30 2310 998032.
E-mail address: ksime@physics.auth.gr (K. Simeonidis).

http://dx.doi.org/10.1016/j.jssc.2014.02.026
0022-4596

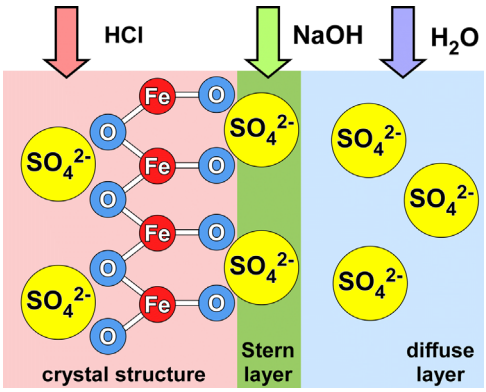

Fig. 1. Schematic representation of the determination steps followed to identify sulfate distribution in iron oxy-hydroxides.

are inorganic or organic, and offers an easy, fast and small sample volume demanding procedure for the determination of routine ions in surface, ground and potable water samples [16]. Based on these techniques, this work describes a combined approach for the separate quantification of sulfates that appear physically sorbed, chemisorbed or incorporated into the crystal structure of solids grown by salt precipitation (Fig. 1). Sequentially, a quantity of powdered solids undergoes leaching in water to release SO_4^{2-} from the diffuse layer, followed by leaching by an alkaline solution to measure sulfates from the Stern layer, and complete acid dissolution to identify those captured within the crystal structure. Iron oxy-hydroxides prepared by the precipitation of $FeSO_4$ at various pH-values were used as test materials. The method was validated by means of X-ray photoelectron and infrared spectroscopy, while the practical possibilities of its use were illustrated by the arsenic removal capacity of the various samples using chemisorbed sulfates.

2. Materials and methods

2.1. Fe oxy-hydroxides preparation

The studied iron oxy-hydroxides were prepared in a laboratory-scale two-stage continuous flow reactor by the precipitation of $FeSO_4 \cdot H_2O$ in aqueous environment at high redox conditions (440–170 mV) in a pH range of 3–12, as described in detail in our previous work [8]. Using this arrangement, instead of a batch reactor it was possible to keep all reaction parameters constant throughout the process. In particular, the high concentration of supplied $FeSO_4$ (40 g/L) implied a proportionally sulfate-rich environment during oxy-hydroxide precipitation. The collected solid suspension was thickened for 24 h in an Imhoff tank and then, the obtained sludge was washed several times with water until equilibrium conductivity reached 2 mS/cm. The sludge was then centrifuged, dried for 4 h at 110 °C, ground and sieved to obtain a fine powder (< 63 μm).

2.2. Determination of SO_4^{2-} in different compartments

2.2.1. Physically sorbed

Free sulfate ions may approach the diffuse layer of the solid's surface and remain in the dried sample to counterbalance the positive surface charge of some materials [17]. This fraction is soluble in water and can be removed by extended washing of the solid. However, thorough washing is not always achieved especially in technological materials and large-scale procedures. Therefore, an extraction step of gently stirring a 20 mg sample with 100 mL distilled water for 15 min and filtration through a 0.45 μm pore-size membrane filter was performed to determine sulfate ions concentration in the filtrate. The measurement was performed by an Alltech 600 ion chromatography system with a Transgenomic ICSep AN1 column using a 1.7 mM $NaHCO_3$/1.8 mM Na_2CO_3 solution as eluent.

2.2.2. Chemisorbed

Another fraction of sulfate ions is strongly coupled to the surface of the oxy-hydroxide in the Stern layer [18]. Since these SO_4^{2-} ions are bound to the metal atoms of the surface, their leaching to the solution requires an alkaline solution. In order to extract the chemically sorbed sulfates, a 20 mg sample was gently stirred with 10 mL of 5 mM NaOH for 15 min, then diluted to 100 mL with distilled water and filtered through a 0.45 μm pore-size membrane filter. The concentration of SO_4^{2-} in the filtrate, which represents the sum of physically and chemisorbed anions, was measured by ion chromatography.

2.2.3. Total content

When sulfate ions participate in the growth of materials a portion of them may be located within the crystal structure and thus, far from the surface. In this case, for their extraction, the grains should be completely dissolved using an acid. Total sulfate content of the oxy-hydroxides was determined gravimetrically by precipitation as $BaSO_4$ [10]. A 200 mg sample was dissolved in 8 mL HCl (6 N) under mild heating. Then, 150 mL of hot distilled water was added, followed by drop-wise addition of 50 mL $BaCl_2$ solution (5 g/L). The white precipitate of $BaSO_4$ was aged under heating for at least 2 h, filtered through a 0.45 μm pore-size fiberglass filter, dried and weighed.

2.3. FT-IR spectroscopy

Fourier-transformed infrared (FT-IR) spectra of the materials were recorded using a Perkin-Elmer Spectrum 100 spectrophotometer. For the measurement, the powdered samples were homogeneously mixed with KBr and pelletized. The spectra obtained were the result of 10 co-added scans with a resolution of 4 cm^{-1}.

2.4. X-ray photoelectron spectroscopy

X-ray photoelectron spectroscopy (XPS) spectra were acquired in an Axis Ultra DLD system by KRATOS. A monochromated Al-*K*α X-ray beam was used as the excitation source. The pass energy was 160 eV for survey scans and 40 eV for high resolution spectra. Each specimen was prepared by pressing powder into a pellet that was then mounted in the holder under ultra-high vacuum. Before measurement, in situ sample cleaning was carried out by ion-etching. During the measurements, the specimens were not charged after a charge neutralizer was applied and calibrated so as the C1*s* peak of adventitious carbon was located at 284.6 eV.

3. Results and discussion

3.1. Development of the analytic procedure

3.1.1. Extraction of physisorbed SO_4^{2-}

The recovery of sulfate ions from the diffuse layer was achieved by the dispersion of a specific quantity of solids in distilled water and mechanical stirring for a sufficient contact time. Therefore, for the optimization of this process in iron oxy-hydroxides, it was necessary to examine the time dependence of measurements and the solid's concentration envelope for reproducible and reliable results. Fig. 2a shows the sulfate ions percentage in the test sample

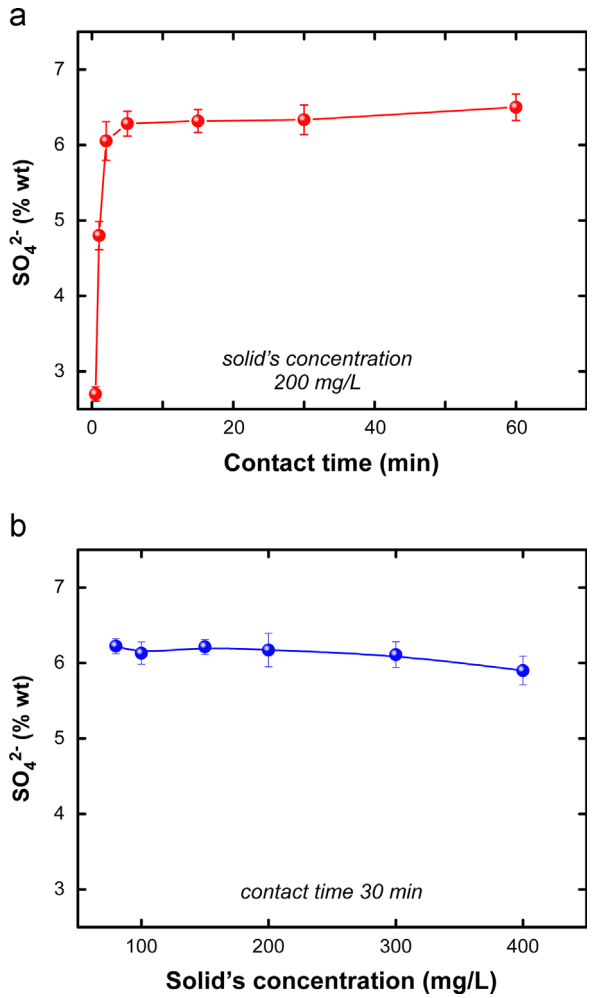

Fig. 2. Effect of contact time (a) and solid's concentration (b) on the determination of sulfates in the diffuse layer in Fe oxy-hydroxide prepared at pH 6.

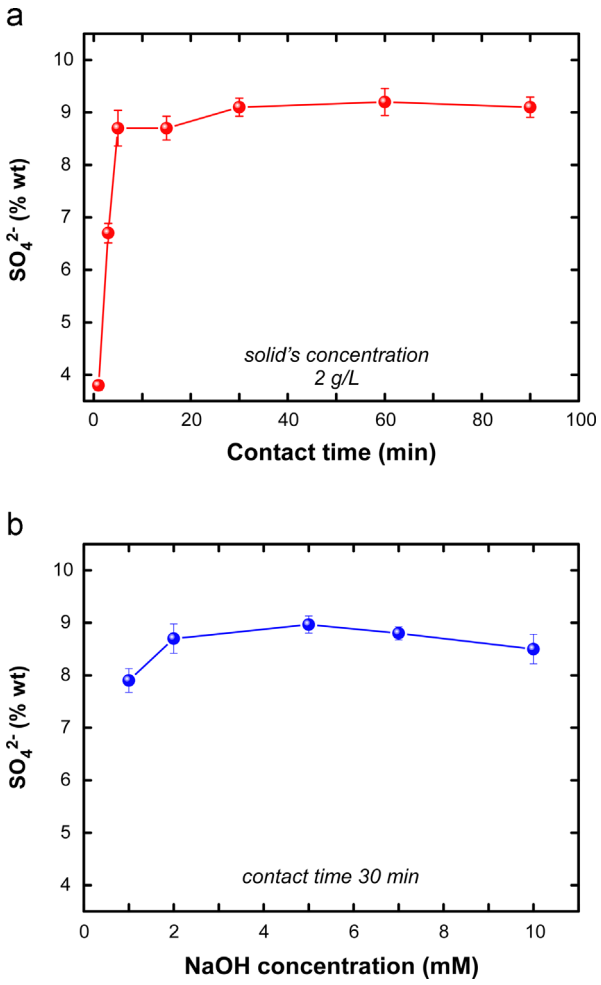

Fig. 3. Effect of contact time (a) and NaOH concentration (b) on the determination of sulfates leached from the diffuse and Stern layers of the Fe oxy-hydroxide prepared at pH 6.

(Fe oxy-hydroxide prepared at pH 6) as determined in the leachate for various contact periods at a concentration of 200 mg/L. It also appears that the steady state (6.4 wt%) was reached in just 2 min whereas statistical analysis verifies the high precision of the method, as the relative standard deviation was well below 5%.

The effect of solid's concentration was evaluated in the range 80–400 mg/L using a contact time of 30 min (Fig. 2b). Obtained values for physisorbed SO_4^{2-} are significantly influenced only by concentrations above 300 mg/L where a decrease of around 5 wt% was observed. According to these results, a contact time of 15 min and a solid's concentration of 200 mg/L were adopted.

3.1.2. *Extraction of chemically sorbed* SO_4^{2-}

Specifically adsorbed sulfate ions may strongly attach onto the surface of the solid (Stern layer) by forming bonds of chemical nature. In order to dissolve this fraction of ions and allow their determination by ion chromatography, washing with an alkaline solution is required. Preliminary experiments showed that the concentration of the applied NaOH solution may significantly modify the extent of SO_4^{2-} extraction or even affect the surface structure of the solid. In particular, low NaOH concentrations result in the partial release of the SO_4^{2-} from the Stern layer whereas higher concentrations may lead to the detachment of iron fines which deteriorate ion chromatography measurements. For this reason, a 20 mg sample was first shaken with 10 mL of NaOH solution and then immediately diluted 10 times with distilled water before filtration.

Evaluation of the optimum parameters was then conducted in the NaOH concentration range 1–10 mM, which corresponds to a pH-range of between 11 and 12, and a contact time of 5–90 min. The results (Fig. 3) showed that NaOH concentrations above 2 mM are adequate to completely leach chemisorbed sulfates. Time evolution of the extraction by applying a 5 mM solution indicates that at least 5 min are required to reach maximum value of released SO_4^{2-} (9.1 wt%) which corresponds to the sum of chemisorbed and physisorbed sulfates. The relative standard deviation of this step of the method was always below 4%. A NaOH concentration of 5 mM and a contact time of 15 min are proposed as optimum.

3.1.3. *Total* SO_4^{2-} *dissolution*

Following the gravimetric method, a colored precipitate of $BaSO_4$ was observed due to FeOOH coprecipitation, when pH was set above 1.5 or when solids mass exceeded 50 mg. To ensure the success of the measurement, a quantity of 200 mg was dissolved in 8 mL of 6 N HCl under mild heating before diluting with distilled water. The reproducibility of this determination step was below 5%.

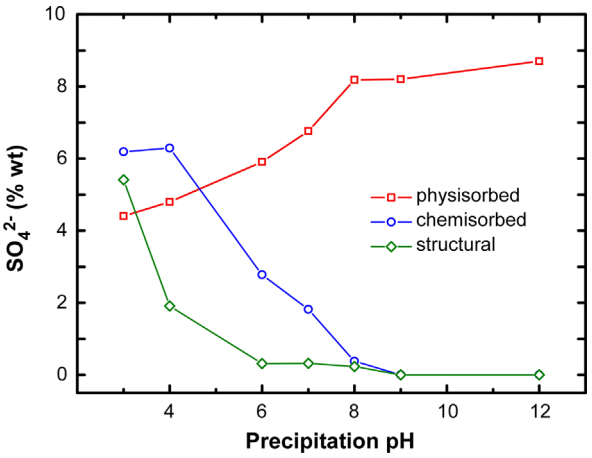

Fig. 4. Distribution of SO_4^{2-} in the crystal structure, diffuse and Stern layers of oxy-hydroxides prepared by precipitation at pH 3–12.

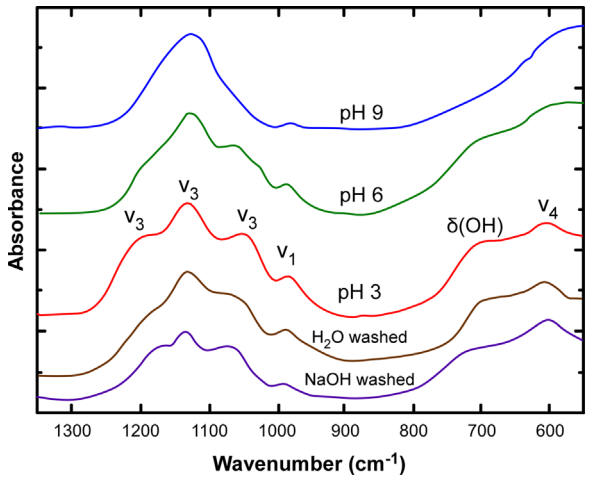

Fig. 5. Representative FT-IR spectra of the iron oxy-hydroxides synthesized at pH 3, 6 and 9 indicating the change of symmetry in SO_4^{2-} species. Corresponding spectra of sample synthesized at pH 3 after extraction by water and NaOH.

3.2. Method application in Fe oxy-hydroxides

To validate the described methodology, the quantitative analysis of SO_4^{2-} distribution in the different compartments of the surface and structure of Fe oxy-hydroxides synthesized at pH 3–12, was performed. Fig. 4 summarizes the results of analysis and calculations which give the percentage in total sample weight of the SO_4^{2-} situated in the diffuse layer, the Stern layer and the structure of the solids. Depending on the acidity of the reaction mixture, the curves can be split into two parts. In the alkaline region, total sulfate content remains constant around 8.5 wt% and lies inclusively in the diffuse layer of the surface. Specifically, for synthesis pH 12, a large fraction of SO_4^{2-} appears in the form of Na_2SO_4 as indicated by the presence of Na (2.5 wt%) in this sample. When precipitation pH decreases below 8, in other words when synthesis takes place below the isoelectric point, a fraction of SO_4^{2-} ions favorably approaches the positively charged solid's surface and form inner or outer sphere complexes, whereas in strong acidic conditions they may even participate in the crystal structure. As previously reported [8], at synthesis pH values below 5, schwertmannite, an Fe oxy-hydroxyl sulfate which incorporates SO_4^{2-} from the environment, is preferable. It should be noted that around one third of the available sulfates may participate in oxy-hydroxide crystals at such low pH values. This shift of SO_4^{2-} from the free state or the diffuse layer to the inner surface and structure is also observed by the gradual increase of total sulfate content that reaches 17 wt% at pH 3, being almost equally distributed as physically adsorbed, chemisorbed or structural.

The existence of these various SO_4^{2-} configurations is also evident by the FT-IR spectra in the mid-infrared region taken from dried samples using the KBr method (Fig. 5). Attenuated total reflection mode experiments (ATR–FTIR) in wet samples indicated that sulfate coordination may vary significantly (conversion of monodentate to bidentate complexes) as a result of proton excess during drying [19,20]. However, in our case, KBr spectra were considered more representative as soon as the technological use of iron oxy-hydroxides in arsenic adsorption requires an extended drying process during preparation. The number of peaks observed between 950 and 1200 cm^{-1}, their relative intensity and position is characteristic of the molecular symmetry and coordination of sulfate ions [21]. Besides, the appearance of a band at around 605 cm^{-1}, assigned to the ν_4 stretching of sulfate anions, is characteristic for structural SO_4^{2-} [22]. In particular, the symmetric stretching ν_1 and the triple asymmetric stretching ν_3 bands may appear as degenerate according to the degree of freedom of the SO_4^{2-} ions. For instance, the case of the oxy-hydroxide prepared at pH 9, where a broad peak corresponding to the degenerate ν_3 band is observed at 1120 cm^{-1}, is explained by the domination of outer sphere complexation ($FeOH_2^+ SO_4^{2-}$ or $FeOH_2^+ HSO_4^-$) which approximates the tetrahedral symmetry of free SO_4^{2-}. These complexes originate from the physisorbed sulfate ions of the diffuse layer and they are stabilized by weak electrostatic interactions or hydrogen bonding. The appearance of a weak ν_1 peak at 980 cm^{-1} is also indicative of partial distortion due to outer sphere complexes.

As the precipitation pH decreases, ν_3 bands gradually split into three peaks and the center of the main peak is shifted to higher wavenumbers (1130 cm^{-1} at pH 3) while the ν_1 stretching becomes more active. This is explained by the lowering in symmetry when sulfate ions, aside from the outer sphere complexes, appear in multiple configurations either by forming inner sphere complexes or by participating in the oxy-hydroxide structure [8]. The splitting into four separate bands is stronger in the spectrum of the oxy-hydroxide synthesized at pH 3. This is consistent with the participation of a significant number of sulfates in inner sphere complexes located on the surface and within the structure of the schwertmannite phase. Specifically, surface complexation of SO_4^{2-} takes place as monodentate or mononuclear/binuclear bidentate, whereas bridging bidentate complexes are favored in the tunnel structure of schwertmannite due to size restrictions, as proposed by Bigham et al. [22]. The existence of structural SO_4^{2-} in this sample is also confirmed by the presence of the ν_4 band.

To correlate findings with chemical analysis results, the FT-IR spectrum was monitored after washing the sample (pH 3) with water and NaOH. Here, the gradual removal of physisorbed and chemisorbed SO_4^{2-} from the schwertmannite's surface causes a lower intensity in the ν_3 absorption band as the contribution of outer sphere and surface inner sphere complexes disappears. However, the fact that intensities of the three ν_3 peaks become comparable combined with the preservation of the ν_4 peak, indicate that structural SO_4^{2-} are the species remaining after the NaOH washing step. The sample synthesized at pH 6 provides another case where a less intense ν_3 splitting occurs while the ν_4 absorption band is absent. It appears that when acidity conditions approach neutral the formation of iron oxy-hydroxyl sulfates such as schwertmannite becomes unfavorable but SO_4^{2-} are still adsorbed as inner sphere and outer sphere complexes on the solid's surface.

X-ray photoelectron spectroscopy investigation of the samples provided further information regarding composition at the solid's

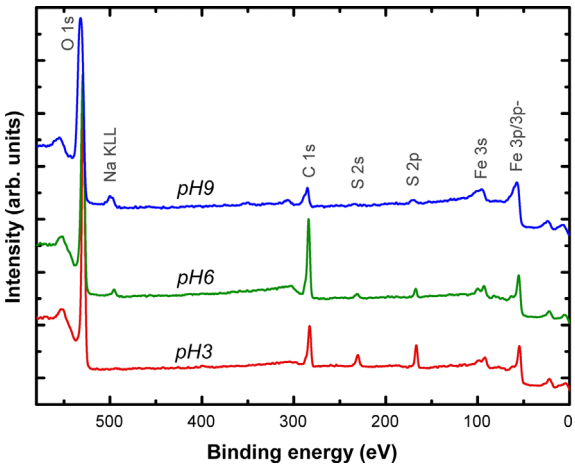

Fig. 6. Wide scan XPS spectra (0–630 eV) of the iron oxy-hydroxides synthesized at pH 3, 6 and 9.

Table 1
Total chemical analysis of iron oxy-hydroxides synthesized at pH 3, 6 and 9 versus results from XPS quantification.

pH	Chemical analysis (wt%)			XPS (wt%*)			
	Fe	S/SO_4^{2-}	Na	Fe	O	S/SO_4^{2-}	Na
3	45.6	5.6/16.9	0.5	56.4	37.1	6.1/18.3	0.4
6	51.4	2.6/7.9	2.7	62.6	33.9	2.3/6.9	1.2
9	51.4	2.4/7.3	4.6	68.3	29.5	1.1/3.3	1.1

* Excluding carbon.

surface (maximum depth 5 nm). Fig. 6 presents the wide scan XPS measurements of Fe oxy-hydroxides precipitated at representative pH values. As the pH increases during synthesis, two important variations are observed in the obtained spectra: the decrease in the intensity of peaks corresponding to sulfur and the gradual enhancement of Na appearance. This, again, proves the tendency of negative-charged sulfate ions to approach sites very close to the solid's surface in acidic conditions whereas the Na^+ cations are favorably adsorbed in strongly alkaline environments.

The quantitative analysis of XPS was performed to provide a better view of SO_4^{2-} configuration on the outer surface layers of studied solids as well as to the inner sphere layer where complexation between iron oxy-hydroxide and SO_4^{2-} may occur. The combination of high specific surface area (50–150 m^2/g) and the very small dimensions of the materials building nanocrystals (<5 nm) [8], also taking into account the inelastic mean free path of the S2*p* photoelectrons that have kinetic energy around 1318 eV [23], allow XPS results to provide a representative view of the chemical features of the nanocrystals. Considering the percentage of SO_4^{2-}, as estimated by the area of XPS S2*p* peaks (Table 1), a continuous rapid drop is observed as pH increases (18.3 wt% at pH 3 becomes 3.3 wt% at pH 9). The results were compared to the total chemical analysis of the materials concerning Fe, SO_4^{2-} and Na after complete dissolution in acid. The decrease of total sulfate content follows an initial loss (from 16.9 wt% at pH 3 to 7.9 wt% at pH 6), but remains constant in the pH range 6–9. This indicates that, in the low pH range, the majority of sulfates in the sample appear in the Stern layer or the structure of oxy-hydroxide and this is in agreement with the results of sulfate determination methodology within the different compartments. By increasing pH, the XPS-determined SO_4^{2-} ions are inversely reduced, since physically sorbed SO_4^{2-} ions lying far from the oxy-hydroxide's surface are not detected. It should be noted that a direct comparison with absolute chemical analysis values should be avoided, since the significant carbon content (5–18 wt%) was excluded from the XPS results, whereas chemical analysis includes the fraction of naturally adsorbed humidity (6–11 wt%).

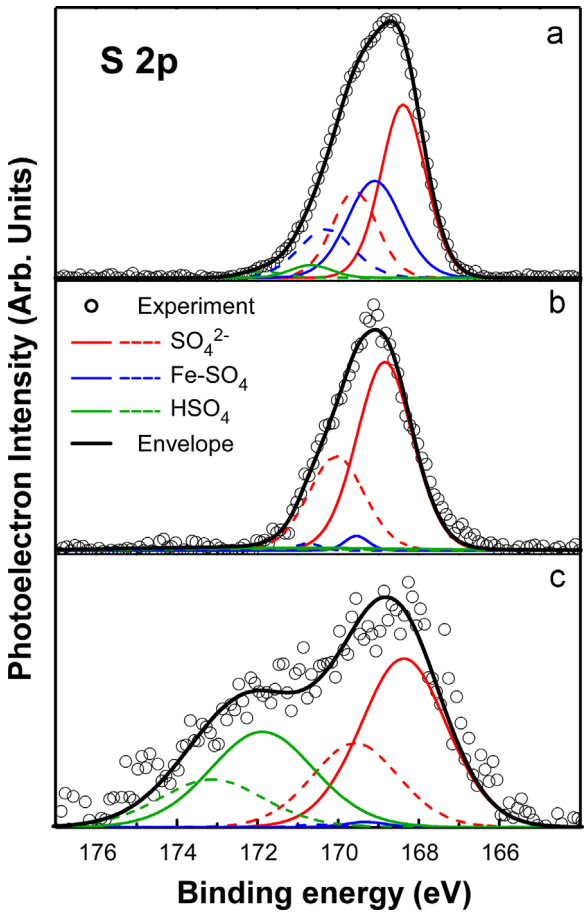

Fig. 7. High resolution XPS spectra of the S2*p* peak for iron oxy-hydroxides synthesized at pH 3, 6 and 9. The spectra were deconvoluted using three doublets corresponding to the $S2p^{1/2}$ (solid lines) and $S2p^{3/2}$ (dashed lines) photoelectron lines for SO_4 (red lines), Fe-SO_4 (blue lines) and HSO_4 (green lines) according to references [24,25]. (For interpretation of the references to color in this figure legend, the reader is referred to the web version of this article.)

Both analytical approaches confirm the presence of large residual Na percentages as a result of the excessive NaOH addition at high pH values. In particular, the contribution of Na^+ may be due to their adsorption on the solid's surface or their crystallization as a separate ionic form with coexisting anions (Na_2SO_4).

To identify the chemical environment and developing bonds of S in the various samples, the S2*p* photoelectron peak was deconvoluted into specific contributions. The S2*p* peak has a fine structure ($S2p^{1/2}$ and $S2p^{3/2}$) due to spin-orbit splitting; thus, each contribution has been fitted by two correlated Lorentzians having 1.2 eV spectral separation, the one ($S2p^{3/2}$) having 50% of the strength of the other ($S2p^{1/2}$) [26]. The particular $S2p^{1/2}$ contributions considered for the deconvolution were: (1) a peak around 168.5 eV (constrained energy for the fitting) corresponding to the binding energy for the free S^{6+} form [24], (2) a peak around 169.5 eV (constrained energy for the fitting) corresponding to Fe-SO_4 complexes [25], and (3) a peak at binding energies higher than 171 eV (free energy for the fitting) that has been proposed to correspond to bisulfate HSO_4 complexes [25]. In Fig. 7, the high resolution XPS spectra of the S2*p* peak for the iron oxy-hydroxides synthesized at pH 3, 6 and 9 are presented. The experimental spectra (open circles) were deconvoluted using three doublets

Table 2
Summary of the results of the XPS S2*p* analysis.

Peak	pH=3		pH=6		pH=9	
	Binding Energy (eV)	*at%*	*Binding Energy (eV)*	*at%*	*Binding Energy (eV)*	*at%*
$S2p^{1/2}$ SO_4	168.4	57.3	168.8	91.4	168.4	58.9
$S2p^{3/2}$ SO_4	169.6		170.0		169.6	
$S2p^{1/2}$ Fe-SO_4	169.2	38.8	169.6	3.0	169.3	0.9
$S2p^{3/2}$ Fe-SO_4	170.4		170.8		170.5	
$S2p^{1/2}$ HSO_4	170.7	3.9	171.0	5.6	171.8	40.2
$S2p^{3/2}$ HSO_4	171.9		172.2		173.0	

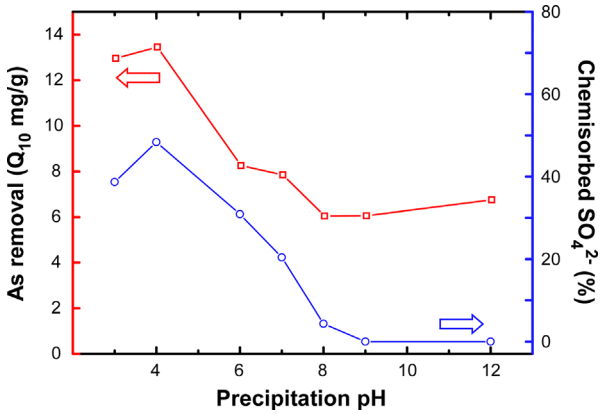

Fig. 8. Adsorption capacity for As(V) at the residual concentration of 10 μg/L compared to the SO_4^{2-} percentage in the Stern layer for Fe oxy-hydroxides synthesized at pH 3–12 (natural water at pH 7).

corresponding to the $S2p^{1/2}$ (solid lines) and $S2p^{3/2}$ (dashed lines) photoelectron lines for sulfate SO_4 (red lines), iron-sulfate Fe-SO_4 (blue lines) and bisulfate HSO_4 (green lines) groups according to references [24,25] and used to identify the relative concentrations of the three types of chemical bonding of S. The results of the XPS S2*p* analysis are summarized in Table 2.

For the oxy-hydroxide prepared at pH 3, a characteristic contribution appears shifted to 169.2 eV and reveals an increase of sulfur oxidation state caused by the strong complexation (bidentate) between SO_4^{2-} and a metal (Fe) through oxygen bridges that causes an electron structure variation and positive charge excess in the side of S. Such an effect is minimal at pH 6 where SO_4^{2-} ions forming lower strengths bonds on solid's surface, dominate. The shift of the main peak to higher energies (168.8 eV) than those expected for symmetrical SO_4^{2-} (168.5) is explained by the monodentate complexation with Fe atoms.

The results are more irregular at the alkaline range, at precipitation pH 9. Apart from the low energy peak, another important contribution appears far shifted to 171.8 eV. This is consistent to the presence of outer sphere bisulfate complexes ($FeOH_2^+ HSO_4^-$) which is amplified in the absence of chemisorbed and structural sulfate forms. The assignment of the shifted shoulder at higher binding energies to protonated bisulfate groups' adsorption (HSO_4^-) has been also suggested elsewhere [25].

3.3. The role of SO_4^{2-} configuration in As removal

To demonstrate the practical importance of the suggested methodology for the design and optimization of technological materials, the arsenic removal efficiency of the tested Fe oxy-hydroxides was correlated to the SO_4^{2-} distribution in their compartments. Fig. 8 shows the As(V) adsorption capacity of these materials at residual concentration equal to the regulation limit for drinking water 10 μg/L (Q_{10}), measured by batch adsorption experiments in natural water adjusted to pH 7. The Q_{10}-value becomes maximum (13.5 mg/g) for adsorbents prepared by precipitation at pH values below 4 and then follows a decreasing trend before becoming almost constant above pH 8 (~7 mg/g). Such variation can be proportionally related to the fraction of chemisorbed SO_4^{2-} located in the Stern layer. This important observation can be explained by the occurrence of an ion-exchange mechanism between As(V) and chemisorbed SO_4^{2-} which is enhanced in samples produced in a positively charged environment (pH < 6). As previously explained [8], in this process the ratio of the released sulfate ions to the captured As(V) was stabilized at around 1:2.5 independently to the initial arsenic concentrations. Therefore, as $H_2AsO_4^-$ approach the solid's surface, chemisorbed SO_4^{2-} favorably leave the surface layer offering new available adsorption sites, each covered by at least one arsenic oxy-anion.

4. Conclusions

The combined implementation of three analytical procedures was presented as a simple route to successfully determinate the different SO_4^{2-} configurations in chemically precipitated solids. In particular, the procedure was optimized to allow the sequential leaching and quantification of sulfate ions from the diffuse layer, the Stern layer and the structure of the solid. Their release from each compartment was achieved by washing in distilled water, in NaOH or dissolving in HCl. To avoid underestimation of sulfate content and overcome possible interferences, the optimum concentrations of solid and solution as well as the appropriate contact times for each step were clarified.

As an example of the method's applicability in materials with technological interest, the distribution of SO_4^{2-} in iron oxy-hydroxides used as arsenic adsorbents was identified and correlated to their synthesis conditions. Results showed that under acidic environments of precipitation, SO_4^{2-} are involved in the formation of the oxy-hydroxide's crystal structure and favor the formation of schwertmannite. Apart from the homogeneously distributed structural SO_4^{2-}, another important fraction is located on the Stern layer as chemisorbed. This arrangement is gradually shifted to the outer surface layers as preparation pH increases. In fact, structural SO_4^{2-} disappear above pH 6 and physically sorbed ones become dominant versus chemisorbed. Beyond previous reports which qualitatively support these findings [5], the current study provides a percentage quantification of SO_4^{2-} distribution.

The accuracy of this methodology was validated by the results of FT-IR and XPS spectroscopy. The different symmetry of multiple sulfate configurations observed by peak splitting at low precipitation pH values turns to degenerate at alkaline conditions, and this is in agreement with the conclusions of similar research [24,27]. Furthermore, more evidence of sulfate complexation on the surface of oxy-hydroxides arises from the positive charge excess in sulfur atoms.

The quantitative determination of SO_4^{2-} can be utilized in the direction of material properties optimization. Here, the improvement of arsenic adsorption efficiency is demonstrated following the percentage of chemisorbed SO_4^{2-}. To prove this conclusion, the removal capacities of iron oxy-hydroxides prepared at pH values 3–12 were compared to the corresponding fraction of SO_4^{2-} located in the Stern layer, and indicate a two-fold performance increase when an ion exchange mechanism between SO_4^{2-} and $H_2AsO_4^-$ oxy-anions is enabled. Similar ion exchange effects have been described for adsorption of mercury and arsenic on iron and aluminum oxy-hydroxides [28,29]. Such analyses may also explain

findings related to the high removal efficiency of arsenic and similar ligands from iron oxy-hydroxyl sulfates such as schwertmannite and jarosite [30,31]. Future work will be carried out to expand the method's applicability for other metal oxides and oxy-hydroxides and elucidate the role of sulfates on the stability of magnetic iron oxide nanoparticles.

Acknowledgments

This work was supported by the European Commission FP7/ Research for SMEs "AquAsZero", Project no.: 232241. K. Simeonidis thanks the Action «Supporting Postdoctoral Researchers» of the Operational Program "Education and Lifelong Learning" (Action's Beneficiary: General Secretariat for Research and Technology), co-financed by the European Social Fund and the Greek State.

References

[1] F. Glombitza, Waste Manag. 21 (2001) 197–203, http://dx.doi.org/10.1016/S0956-053X(00)00061-1.
[2] A.S. Sheoran, V. Sheoran, R.P. Choudhary, Miner. Eng. 23 (2010) 1073–1100, http://dx.doi.org/10.1016/j.mineng.2010.07.001.
[3] J. Subrt, V. Stengl, S. Bakardjieva, L. Szatmary, Powder Technol. 169 (2006) 33–40, http://dx.doi.org/10.1016/j.powtec.2006.07.009.
[4] A. Pilarska, M. Wysokowski, E. Markiewicz, T. Jesionowski, Powder Technol. 235 (2013) 148–157, http://dx.doi.org/10.1016/j.powtec.2012.10.008.
[5] J. Majzlan, S.C.B. Myneni, Environ. Sci. Technol. 39 (2005) 188–194, http://dx.doi.org/10.1021/es049664p.
[6] R.P.J.J. Rietra, T. Hiemstra, W.H. Van Riemsdijk, J. Colloid Interface Sci. 218 (1999) 511–521, http://dx.doi.org/10.1006/jcis.1999.6408.
[7] J. Gimenez, M. Martinez, J. de Pablo, M. Rovira, L. Duro, J. Hazard. Mater. 141 (2007) 575–580, http://dx.doi.org/10.1016/j.jhazmat.2006.07.020.
[8] S. Tresintsi, K. Simeonidis, G. Vourlias, G. Stavropoulos, M. Mitrakas, Water Res. 46 (2012) 5255–5267, http://dx.doi.org/10.1016/j.watres.2012.06.049.
[9] K. Fukushi, D. Sverjensky, Geochim. Cosmochim. Acta 71 (2007) 1–24, http://dx.doi.org/10.1016/j.gca.2006.08.048.
[10] J. Mendham, R.C. Denney, J.D. Barnes, M.J.K. Thomas, Vogel's Quantitative Chemical Analysis, sixth ed., Prentice Hall, Essex, England, 2000.
[11] K.W. Irwin, L.M. Lavkulich, Commun. Soil Sci. Plant Anal. 28 (1997) 561–570, http://dx.doi.org/10.1080/00103629709369811.
[12] R. Goguel, Anal. Chem. 41 (1969) 1034, http://dx.doi.org/10.1021/ac60277a011.
[13] W. Frenzel, A. Rauterberg, Microchim. Acta 106 (1992) 175–182, http://dx.doi.org/10.1007/BF01242088.
[14] M. Amin, L.W. Lim, T. Takeuchi, J. Chromatogr. A 1182 (2008) 169–175, http://dx.doi.org/10.1016/j.chroma.2008.01.007.
[15] K. Fukusi, T. Sato, N. Yanase, Environ. Sci. Technol. 37 (2003) 3581–3586, http://dx.doi.org/10.1021/es026427i.
[16] P. Miskaki, E. Lytras, L. Kousouris, P. Tzoumerkas, Desalination 213 (2007) 182–188, http://dx.doi.org/10.1016/j.desal.2006.05.063.
[17] T. Hiemstra, W.H. Van Riemsdijk, J. Colloid Interface Sci. 301 (2006) 1–18, http://dx.doi.org/10.1016/j.jcis.2006.05.008.
[18] R. Rahnemaie, T. Hiemstra, W.H. Van Riemsdijk, J. Colloid Interface Sci. 297 (2006) 379–388, http://dx.doi.org/10.1016/j.jcis.2005.11.003.
[19] G. Lefevre, Adv. Colloid Interface Sci. 107 (2004) 109–123, http://dx.doi.org/10.1016/j.cis.2003.11.002.
[20] S.J. Hug, J. Colloid Interface Sci. 188 (1997) 415–422, http://dx.doi.org/10.1006/jcis.1996.4755.
[21] G.Y. Zhang, D. Peak, Geochim. Cosmochim. Acta 71 (2007) 2158–2169, http://dx.doi.org/10.1016/j.gca.2006.12.020.
[22] J.M. Bigham, U. Schwertmann, L. Carlson, E. Murad, Geochim. Cosmochim. Acta 54 (1990) 2743–2758, http://dx.doi.org/10.1016/0016–7037(90)90009-A.
[23] M.P. Seah, W.A. Dench, Surf. Interface Anal. 1 (1979) 2–11, http://dx.doi.org/10.1002/sia.740010103.
[24] B. Stypula, J. Stoch, Corros. Sci. 36 (1994) 2159–2167, http://dx.doi.org/10.1016/0010-938X(94)90014-0.
[25] J. Baltrusaitis, D.M. Cwiertny, V.H. Grassian, Phys. Chem. Chem. Phys. 9 (2007) 5542–5554, http://dx.doi.org/10.1039/b709167b.
[26] A. Bierla, G. Fromentin, C. Minfray, J.-M. Martin, T. Le Mogne, N. Genet, Wear 286–287 (2012) 116–123, http://dx.doi.org/10.1016/j.wear.2011.05.007.
[27] M. Zhu, P. Northrup, C. Shi, S.J.L. Billinge, D.L. Sparks, G.A. Waychunas, Environ. Sci. Technol. Lett. 1 (2014) 97, http://dx.doi.org/10.1021/ez400052r.
[28] C.S. Kim, J.J. Rytuba, G.E. Brown , J. Colloid Interface Sci. 270 (2004) 9–20, http://dx.doi.org/10.1016/j.jcis.2003.07.029.
[29] Y. Jia, G.P. Demopoulos, Environ. Sci. Technol. 39 (2005) 9523–9527, http://dx.doi.org/10.1021/es051432i.
[30] M. Grafe, D.A. Beattie, E. Smith, W.M. Skinner, B. Singh, J. Colloid Interface Sci. 322 (2008) 399–413, http://dx.doi.org/10.1016/j.jcis.2008.02.044.
[31] J. Antelo, S. Fiol, D. Gondar, R. Lopez, F. Arce, J. Colloid Interface Sci. 386 (2012) 338–343, http://dx.doi.org/10.1016/j.jcis.2012.07.008.